Miniaturized probe for femtosecond laser microsurgery and two-photon imaging

Christopher L. Hoy[1], Nicholas J. Durr[2], Pengyuan Chen[1], Wibool Piyawattanametha[3], Hyejun Ra[3], Olav Solgaard[3], and Adela Ben-Yakar[1,2,*]

[1]Department of Mechanical Engineering, The University of Texas at Austin, Austin, TX 78712
[2]Department of Biomedical Engineering, The University of Texas at Austin, Austin, TX 78712
[3]Department of Electrical Engineering, Stanford University, Stanford, CA 945305
**Corresponding author: ben-yakar@mail.utexas.edu*

Abstract: Combined two-photon fluorescence microscopy and femtosecond laser microsurgery has many potential biomedical applications as a powerful "seek-and-treat" tool. Towards developing such a tool, we demonstrate a miniaturized probe which combines these techniques in a compact housing. The device is 10 × 15 × 40 mm^3 in size and uses an air-core photonic crystal fiber to deliver femtosecond laser pulses at 80 MHz repetition rate for imaging and 1 kHz for microsurgery. A fast two-axis microelectromechanical system scanning mirror is driven at resonance to produce Lissajous beam scanning at 10 frames per second. Field of view is 310 µm in diameter and the lateral and axial resolutions are 1.64 µm and 16.4 µm, respectively. Combined imaging and microsurgery is demonstrated using live cancer cells.

OCIS Codes: (190.4180) Multiphoton Processes; (170.1020) Tissue Ablation; (170.2150) Endoscopic Imaging.

References and links

1. U. K. Tirlapur and K. König, "Targeted transfection by femtosecond laser," Nature **418**, 290-291 (2002).
2. M. F. Yanik, H. Cinar, H. N. Cinar, A. D. Chisholm, Y. S. Jin, and A. Ben-Yakar, "Functional regeneration after laser axotomy," Nature **432**, 822-822 (2004).
3. A. Vogel, J. Noack, G. Hüttman, and G. Paltauf, "Mechanisms of femtosecond laser nanosurgery of cells and tissues," Appl. Phys. B **81**, 1015-1047 (2005).
4. N. Shen, D. Datta, C. B. Schaffer, P. LeDuc, D. E. Ingber, and E. Mazur, "Ablation of cytoskeletal filaments and mitochondria in live cells using a femtosecond laser nanoscissor," Mech. Chem. Biosyst. **2**, 17-25 (2005).
5. A. A. Oraevsky, L. B. Da Silva, A. M. Rubenchik, M. D. Feit, M. E. Glinsky, M. D. Perry, B. Mammini, M., W. Small, IV, and B. C. Stuart, "Plasma mediated ablation of biological tissues with nanosecond-to-femtosecond laser pulses: Relative role of linear and nonlinear absorption," IEEE J. Sel. Top. Quantum Electron. **2**, 801-809 (1996).
6. I. Ratkay-Traub, I. E. Ferincz, T. Juhasz, R. M. Kurtz, and R. R. Krueger, "First clinical results with the femtosecond neodynium-glass laser in refractive surgery," J. Refract. Surg. **19**, 94-103 (2003).
7. W. Denk, J. H. Strickler, and W. W. Webb, "2-photon laser scanning fluorescence microscopy," Science **248**, 73-76 (1990).
8. P. T. C. So, C. Y. Dong, B. R. Masters, and K. M. Berland, "Two-photon excitation fluorescence microscopy," Annu. Rev. Biomed. Eng. **2**, 399-429 (2000).
9. W. R. Zipfel, R. M. Williams, and W. W. Webb, "Nonlinear magic: Multiphoton microscopy in the biosciences," Nat. Biotechnol. **21**, 1368-1376 (2003).
10. P. Theer and W. Denk, "On the fundamental imaging-depth limit in two-photon microscopy," J. Opt. Soc. Am. A **23**, 3139-3149 (2006).
11. P. Theer, M. Hasan, and W. Denk, "Two-photon imaging to a depth of 1000µm in living brains by use of a Ti:Al_2O_3 regenerative amplifier," Opt. Lett. **28**, 1022-1024 (2003).
12. N. Nishimura, C. B. Schaffer, B. Friedman, P. S. Tsai, P. D. Lyden, and D. Kleinfeld, "Targeted insult to subsurface cortical blood vessels using ultrashort laser pulses: Three models of stroke," Nature Methods **3**, 99-108 (2006).
13. K. König, O. Krauss, and I. Riemann, "Intratissue surgery with 80 MHz nanojoule femtosecond laser pulses in the near infrared," Opt. Express **10**, 171-176 (2002).

#95706 - $15.00 USD Received 2 May 2008; revised 8 Jun 2008; accepted 10 Jun 2008; published 20 Jun 2008

14. E. Zeira, A. Manevitch, A. Khatchatouriants, O. Pappo, E. Hyam, M. Darash-Yahana, E. Tavor, A. Honigman, A. Lewis, and E. Galun, "Femtosecond infrared laser—an efficient and safe in vivo gene delivery system for prolonged expression," Mol. Ther. **8**, 342-350 (2003).
15. L. Sacconi, I. M. Tolic´-Nørrelykke, R. Antolini, and F. S. Pavone, "Combined intracellular three-dimensional imaging and selective nanosurgery by a nonlinear microscope," J. Biomed. Opt. **10**, 014002-014001 - 014002-014005 (2005).
16. K. König, I. Riemann, F. Stracke, and R. Le Harzic, "Nanoprocessing with nanojoule near-infrared femtosecond laser pulses," Med. Las. Appl. **20**, 169-184 (2005).
17. F. Helmchen, M. S. Fee, D. W. Tank, and W. Denk, "A miniature head-mounted two-photon microscope: High-resolution brain imaging in freely moving animals," Neuron **31**, 903-912 (2001).
18. J. C. Jung and M. J. Schnitzer, "Multiphoton endoscopy," Opt. Lett. **28**, 902-904 (2003).
19. W. Göbel, J. N. D. Kerr, A. Nimmerjahn, and F. Helmchen, "Miniaturized two-photon microscope based on a flexible coherent fiber bundle and a gradient-index lens objective," Opt. Lett. **29**, 2521-2523 (2004).
20. B. A. Flusberg, J. C. Jung, E. D. Cocker, E. P. Anderson, and M. J. Schnitzer, "*In vivo* brain imaging using a portable 3.9 gram two-photon fluorescence microendoscope," Opt. Lett. **30**, 2272-2274 (2005).
21. M. T. Myaing, D. J. MacDonald, and X. Li, "Fiber-optic scanning two-photon fluorescence endoscope," Opt. Lett. **31**, 1076-1078 (2006).
22. L. Fu, A. Jain, C. Cranfield, H. Xie, and M. Gu, "Three-dimensional nonlinear optical endoscopy," JBO Lett. **12**, 0405011-04050113 (2007).
23. K. König, A. Ehlers, I. Riemann, S. Schenkl, R. Bückle, and M. Kaatz, "Clinical two-photon microendoscopy," Microsc. Res. Tech. **70**, 398-402 (2007).
24. D. Lee and O. Solgaard, "Two-axis gimbaled microscanner in double SOI layers actuated by self-aligned vertical electrostatic combdrive" in *Proceedings of the Solid-State Sensors, Actuators and Microsystems Workshop, Hilton Head Island*, Hilton Head Island, South Carolina, June 6-10, 2004, 352-355.
25. H. Ra, W. Piyawattanametha, Y. Taguchi, D. Lee, M. J. Mandella, and O. Solgaard, "Two-dimensional MEMS scanner for dual-axes confocal microscopy," J. Microelectromech. Syst. **16**, 969-976 (2007).
26. W. Piyawattanametha, R. P. J. Barretto, T. H. Ko, B. A. Flusberg, E. D. Cocker, H. Ra, D. Lee, O. Solgaard, and M. J. Schnitzer, "Fast-scanning two-photon fluorescence imaging based on a microelectromechanical systems two-dimensional scanning mirror," Opt. Lett. **31**, 2018-2020 (2006).
27. K. C. Maitland, H. J. Shin, H. Ra, D. Lee, O. Solgaard, and R. Richards-Kortum, "Single fiber confocal microscope with a two-axis gimbaled MEMS scanner for cellular imaging," Opt. Express **14**, 8604-8612 (2006).
28. J. B. Guild, C. Xu, and W. W. Webb, "Measurement of group delay dispersion of high numerical aperture objective lenses using two-photon excited fluorescence," Appl. Opt. **36**, 397-401 (1997).
29. D. L. Dickensheets and G. S. Kino, "Micromachined scanning confocal optical microscope," Opt. Lett. **21**, 764-766 (1996).
30. M. M. Dickens, M. P. Houlne, S. Mitra, and D. J. Bornhop, "Method for depixelating micro-endoscopic images," Opt. Eng. **38**, 1836-1842 (1999).
31. J. W. Goodman, *Introduction to Fourier Optics,* 3rd Edition (Roberts & Co., Englewood, 2005).
32. B. A. Flusberg, E. D. Cocker, W. Piyawattanametha, J. C. Jung, E. L. M. Cheung, and M. J. Schnitzer, "Fiber-optic fluorescence imaging," Nature Methods **2**, 941-950 (2005).
33. F. Bourgeois and A. Ben-Yakar, "Femtosecond laser nanoaxotomy properties and their effect on axonal recovery in *C. Elegans*," Opt. Express **15**, 8521-8531 (2007).
34. Urey, H., "Spot size, depth-of-focus, and diffraction ring intensity formulas for truncated Gaussian beams," Appl. Opt., **43** 620-625 (2004)
35. K. König, P. T. C. So, W. W. Mantulin, and E. Gratton, "Cellular response to near-infrared femtosecond laser pulses in two-photon microscopes " Opt. Lett. **22**, 135-136 (1997).
36. K. König, T. W. Becker, P. Fischer, I. Riemann, and K. J. Halbhuber, "Pulse-length dependence of cellular response to intense near-infrared laser pulses in multiphoton microscopes," Opt. Lett. **24**, 113-115 (1999).
37. H. J. Koester, D. Baur, R. Uhl, and S. W. Hell, "Ca^{2+} fluorescence imaging with pico- and femtosecond two-photon excitation: Signal and photodamage," Biophys. J. **77**, 2226-2236 (1999).
38. A. Hopt and E. Neher, "Highly nonlinear photodamage in two-photon fluorescence microscopy," Biophys. J. **80**, 2029-2036 (2001).
39. H. F. Wang, T. B. Huff, D. A. Zweifel, W. He, P. S. Low, A. Wei, and J. X. Cheng, "In vitro and in vivo two-photon luminescence imaging of single gold nanorods," Proc. Natl. Acad. Sci. U. S. A. **102**, 15752-15756 (2005).
40. N. J. Durr, T. Larson, D. K. Smith, B. A. Korgel, K. Sokolov, and A. Ben-Yakar, "Two-photon luminescence imaging of cancer cells using molecularly targeted gold nanorods," Nano Lett. *7*, 941-945 (2007).
41. M. J. Mandella, J. T. C. Liu, W. Piyawattanametha, H. Ra, P.-L. Hsiung, L. K. Wong, O. Solgaard, T. D. Wang, C. H. Contag, and G. S. Kino, "Compact optical design for dual-axes confocal endoscopic microscopes," Proc. SPIE **6443**, E1-E9 (2007).

#95706 - $15.00 USD Received 2 May 2008; revised 8 Jun 2008; accepted 10 Jun 2008; published 20 Jun 2008

1. Introduction

In recent years, femtosecond laser microsurgery (FLMS) has emerged as a superior technique for ablation of cells and subcellular structures and offers the highest precision for microsurgery in three-dimensional (3D) tissue [1-4]. In FLMS, laser absorption is confined to the focal volume as a result of nonlinear interactions. The high peak intensities and short time duration of the pulses lead to efficient and rapid ionization of tissue before energy can be lost to heat diffusion. As a result, femtosecond lasers require much less energy for ablation and lead to significantly less heating of surrounding tissue (especially for repetition rates < 1 MHz) when compared to ablation with nanosecond or longer duration laser pulses [3, 5]. Owing to these advantages, FLMS has been gradually moving from the laboratory to the physician's office, most notably in ophthalmology, where femtosecond laser systems produced by IntraLase Corp. have been clinically used for LASIK surgery since 2003 [6].

To fully realize the potential of FLMS in many clinical applications, however, it must be guided and monitored by an equally precise and penetrating 3D imaging technique, such as two-photon microscopy (TPM) [7-9]. Two-photon microscopy utilizes near infrared (NIR) femtosecond laser pulses similar to FLMS and provides similar advantages, such as inherent optical sectioning and penetration depth in excess of 1 mm [10, 11]. By combining FLMS with TPM, physicians can guide precise surgical tools with microscopic imaging capabilities deep inside scattering tissue. Indeed, the use of femtosecond lasers for both imaging and manipulation of biological samples has been demonstrated in laboratory settings using large table-top systems [12-16]. This combined tool can be used for diagnosis and treatment of various diseases as well as for *in vivo* monitoring of disease progression.

Many potential clinical applications of FLMS and TPM require packaging these systems in a small and flexible device. Miniaturized two-photon microscopy probes have been developed since 2001 [17], primarily for neurological research [18-20], though recently probes have been developed toward clinical examination of diseased tissue [21, 22]. To date, there have been no known flexible probes for FLMS, due to the difficulties of delivering high peak intensities through optical fibers and miniature optics caused by nonlinear effects and material damage. In this work, we present a new miniaturized probe that addresses these challenges and serves as a first step towards a clinical TPM/FLMS endoscope.

2. Results

2.1 Probe design

The design of the probe, shown in Fig. 1, enables both nonlinear optical imaging and microsurgery. The major components of the probe are an air-core photonic crystal fiber (PCF) (Fig. 1(c)), two-axis microelectromechanical systems (MEMS) scanning mirror (Fig. 1(d)), miniature relay lens system, and gradient index (GRIN) objective lens. These components provide the advantages of compact size and the ability to handle high peak intensity laser pulses to enable FLMS and TPM in a miniaturized system. This design uses the same optical pathways for both microsurgery and fluorescence excitation, thus providing visualization and guidance at the exact location of ablation. Though several of these optical components have been utilized in previous miniature two-photon microscope designs, the incorporation of amplified high peak-intensity pulses for microsurgery led to a design that not only enables FLMS, but it improves imaging capabilities as well. Specifically, (1) the air-core fiber allows delivery of high peak intensity femtosecond pulses for microsurgery, (2) the relay lenses image the scanning mirror to the back aperture of the objective lens, thus providing a large field of view (FOV) with uniform excitation, (3) the use of individual relay lenses avoids the internal foci that occur in multiple pitch length GRIN relay lenses, thus allowing for delivery of high peak intensities without material damage [23], (4) the relay lenses also expand the beam, thus allowing the use of a small and fast MEMS scanning mirror for high frame rates, while still overfilling the objective lens aperture for improved resolution, (5) both axes of the

#95706 - $15.00 USD Received 2 May 2008; revised 8 Jun 2008; accepted 10 Jun 2008; published 20 Jun 2008

MEMS scanner are driven at resonance, allowing the use of low driving voltages to scan large FOV, and (6) the collection pathway is separated from the excitation fiber and uses a large numerical aperture (NA) fiber, providing improved collection efficiency.

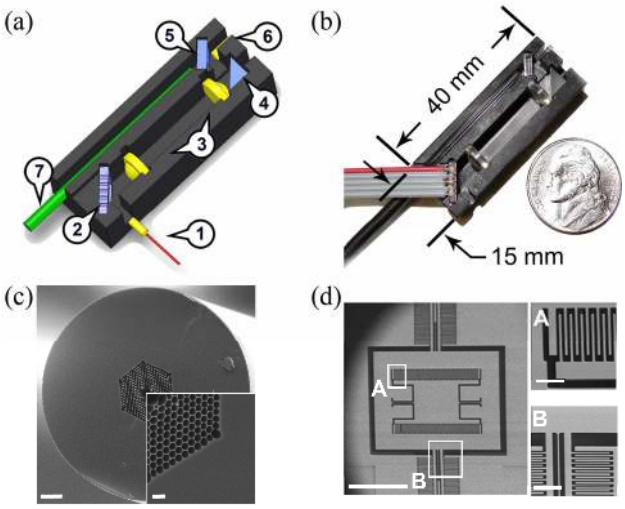

Fig. 1. The 10 × 15 × 40 mm^3 miniaturized two-photon microscope and femtosecond laser microsurgery probe. (a) The model includes 1) air-core PCF and GRIN collimating lens, 2) two-axis MEMS scanner, 3) miniature aspheric relay lenses, 4) mirror, 5) dichroic mirror, 6) 0.46-NA GRIN objective lens, and 7) 2mm-core plastic optical fiber. (b) The photograph shows the miniature probe as built without the delivery fiber and the lid that was used to seal the probe. The PCF and its collimating GRIN lens were mounted separately and aligned to the probe during experiments. (c) SEM micrographs of the PCF core and cladding structure, and MEMS scanning mirror design (d). The scale bars are 15 µm in (c) (3 µm in inset), and 600 µm in (d) (120 µm in inset).

An air-core PCF (one meter long, Air-6-800, Crystal Fiber A/S) delivers femtosecond pulses for both imaging and microsurgery into a 10 × 15 × 40 mm^3 Delrin® housing (see Fig. 1(c)). Pulses for imaging (at 80 MHz repetition rate from Mai Tai, Spectra Physics) were delivered at the minimum-dispersion wavelength of the PCF near 753 nm. The pulse duration was measured to be 152 fs after the fiber for a 117 fs input pulse duration using a homebuilt interferometric autocorrelator. Pulses for microsurgery (at 1 kHz repetition rate from Spitfire, Spectra Physics) were delivered near 780 nm, the operation wavelength of the chirped pulse amplifier. Microsurgery pulses were prechirped using the compressor in the amplifier to compensate for the fiber dispersion at this wavelength, resulting in a pulse duration of 178 fs exiting the fiber. The beam coming out of the fiber was collimated by a gradient index (GRIN) lens (0.46 NA, 1.8 mm diameter). The fiber tip and its collimating lens were held in a micropositioning stage that was aligned to send the collimated laser beam into the probe housing.

The laser beam is scanned inside the probe housing using a two-axis gimbal MEMS scanning mirror driven by vertical electrostatic combdrives (see Fig. 1(d)) [24, 25]. The reflective surface of this mirror is bare silicon, which provides a reflectance of ~30%. The 500 × 500 µm^2 mirror exhibits resonance frequencies of 1.54 kHz and 2.73 kHz. Maximum optical beam deflections of ±10.5° for the outer axis and ±10° for the inner axis are achieved by driving the mirrors with sinusoidal voltage signals at their resonant frequencies using peak voltage values of 80 volts. The corresponding number of resolvable spots, a key figure of merit for scanning devices, is approximately 172 x 232 for this device [26, 27]. The collimated beam on the scanning mirror is imaged onto the back aperture of a GRIN lens

#95706 - $15.00 USD Received 2 May 2008; revised 8 Jun 2008; accepted 10 Jun 2008; published 20 Jun 2008

(0.46 NA, 210 μm working distance, and 1.8 mm diameter) through an aspherical lens pair which also serves as a 3.4× beam expander. The total group delay dispersion contribution from the miniature optics in the probe is estimated to be ~1230 fs^2, similar to that of standard microscope objectives used in two-photon microscopy [28].

Maximum power that could be delivered at the sample is limited to 120 mW near the 753 nm imaging wavelength. The total transmission efficiency of the probe is about 12% as a result of a ~65% coupling efficiency of the fiber, the ~30% reflectance of the MEMS mirror, and the insertion losses of the remaining optics. For the microsurgery laser, the maximum pulse energy deliverable to the sample was found to be 350 nJ, above which the laser intensity at the entrance to the photonic crystal fiber began to damage the fiber and decrease coupling efficiency. The power at the sample for both lasers can be increased in the future through use of a metallic-coated MEMS mirror. The deliverable energy of the microsurgery laser can also be increased in the future through additional pre-chirping, thus decreasing further the peak laser intensity during fiber coupling.

Fluorescence emission is collected by a 2-mm core plastic optical fiber (0.51 NA). The collection fiber is positioned directly behind a 5 × 5 mm^2 dichroic mirror which reflects wavelengths above 715 nm. The collected fluorescence is delivered through 1 meter of the fiber and focused into a photomultiplier tube (H7422-40, Hamamatsu) by a 4 mm focal length lens with a Schott BG38 filter blocking scattered laser light.

For imaging, the laser beam is scanned in a Lissajous pattern by a LabView® program driving both axes of the MEMS mirror at resonant frequencies with sinusoidal voltage signals [17, 20, 29]. The emission signal is collected at 1 MHz rate (1 μs dwell time per pixel) and processed in real-time to display a 256 × 256 pixel image at 10 frames per second (fps). The program also incorporates a variable pixel delay to compensate for phase delay between the driving voltage and the acquired signal, as well as phase delay between mirror axes. Further improvement of the images can be achieved during post-processing through frame averaging and spatial filtering. Low-pass spatial filtering using a fast Fourier transform (FFT) algorithm and a 1.2 cycles/μm cut-off frequency in the *x* and *y* directions effectively eliminates isolated pixels which are not sampled during the Lissajous scan and appear as sub-resolution zero-value pixels aligned in vertical and horizontal rows in the center of the image [30, 31]. The cut-off frequency was based on the measured resolution of the system, so as to not filter out any useful signal, similar to the filtering implemented in Dickens *et al.* [30]

2.2 Imaging characterization

The size and curvature of the FOV was investigated by imaging 1 μm fluorescent beads (Invitrogen) deposited onto a microscope slide. This provided a fairly uniform and flat sample, which was translated by piezoelectric stages in the *x* and *y* directions during imaging to calibrate image scale. Using peak driving voltage to the MEMS between 20 - 80 volts, the diameter of the FOV could be varied between 36 - 310 μm. The maximum FOV is shown in Fig 2(a). The limiting aperture for the maximum FOV was found to be the clear aperture of the second relay lens in the beam path. We observed a fairly constant intensity over much of the field.

#95706 - $15.00 USD Received 2 May 2008; revised 8 Jun 2008; accepted 10 Jun 2008; published 20 Jun 2008

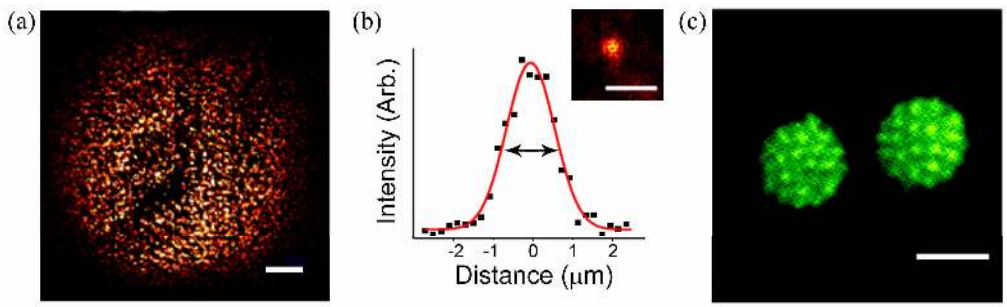

Fig. 2. Two-photon fluorescence imaging characterization of the miniature TPM/FLMS probe. (a) 1 μm fluorescent beads on glass, demonstrating 310 μm maximum FOV. Laser power at the sample was measured to be 8.2 mW. (b) A representative lateral point spread function from 100 nm fluorescent beads in agar (shown in inset). Black dots represent measured intensity values while the red line is the Gaussian curve fit. (c) Pollen grains imaged using 9.0 mW average power at the sample. Image (a) is averaged over 0.6 seconds, while images (b) and (c) are averaged over 5 seconds, all at 10 fps. Images (a) and (c) were spatially filtered. Scale bars are 50 μm in (a), 5 μm in (b), and 25 μm in (c).

The resolution of the probe was measured experimentally by imaging 100 nm fluorescent beads (Invitrogen) in an agar gel across a 100 μm FOV to obtain the 3D two-photon point-spread function (PSF). The full widths at half-maximum of the Gaussian fits to the bead images (Fig. 2(b)) were found to be 1.64±0.09 μm and 16.4±1.0 μm, for lateral and axial dimensions, respectively. The measurements were averaged across 10 beads and the reported errors correspond to the standard error of the mean. The extended axial resolution has been previously attributed to spherical aberration from the GRIN lens and is similar to what has been observed in other studies [19-22, 32].

Using the probe, two-photon images of fluorescently-labeled pollen grains (30-4264, Carolina Biological Supply Co.) were used to demonstrate the resolving power of probe at the micrometer scale, and can be seen in Fig. 2(c).

2.3 Cellular imaging and microsurgery

The combined imaging and microsurgery capabilities of the probe were demonstrated using breast carcinoma cells (MDMBA468) grown in a single cell layer and labeled with the fluorescent cell viability dye, calcein AM. During these experiments, the cells were imaged before and immediately following ablation. For microsurgery, the flipping mirror that directs the imaging beam was lowered to direct the microsurgery beam into the fiber while the imaging laser was blocked. The MEMS mirror was static and undeflected during microsurgery, thus targeting the center of the FOV. By bringing the microsurgery beam collinearly with the imaging beam and triggering it through the imaging program, simultaneous imaging and microsurgery of off-axis targets is also possible with this system.

Figures 3(a) and 3(b) present two-photon images before and after femtosecond laser microsurgery with a single pulse at 280 nJ pulse energy. Ablation of the targeted cell is evidenced by the loss of its fluorescence signal, where the abrupt signal loss suggests that the membrane of the targeted cell was ruptured, releasing all of the calcein dye. In this set of experiments, the pulse energy was increased incrementally from 160 nJ until loss of cellular fluorescence was observed at 280 nJ. Ablation using this energy level was found to be very repeatable. As only a single laser pulse was used in this experiment, we expect that the loss in fluorescence is due to ablation rather than photobleaching of the calcein inside the cell. Because the cells are much larger (~15-20 μm diameter) than the focal spot, longer exposures would be necessary to photobleach the total volume of the cell. Note that the high precision of fs-laser ablation allowed disintegration of the target cell while adjacent cells remain intact.

#95706 - $15.00 USD Received 2 May 2008; revised 8 Jun 2008; accepted 10 Jun 2008; published 20 Jun 2008

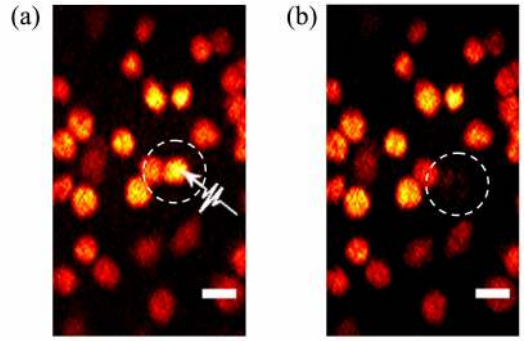

Fig. 3. Combined two-photon microscopy and femtosecond laser microsurgery of a single layer of breast carcinoma cells. (a) Two photon image of a single layer of live breast carcinoma cells after uptake of calcein AM taken prior to irradiation with high intensity pulses. (b) The same FOV as (a), immediately after irradiation with a single pulse at 280 nJ pulse energy. Average laser power used for imaging in both images was 10 mW. Both images were averaged over 5 seconds at 10 fps and spatially filtered. Note that the targeted cell has lost fluorescence while the cell touching the targeted cell is left intact. Scale bars are 20 μm.

We also investigated two-photon imaging and ablation of cells within a three-dimensional (3D) tissue phantom consisting of breast carcinoma cells embedded in a collagen matrix. Cells were labeled using calcein AM and imaged using 17 mW average power measured at the sample. Axial steps of 6.6 μm were made by moving the sample on a piezoelectric stage. Figure 4 presents images where a cell approximately 125 μm deep was targeted for ablation. Here, 5000 pulses at 213 nJ per pulse were used as the scattering collagen media reduces the total energy reached to the focal plane. In this case, we again observed the immediate loss of cellular fluorescence after irradiation with the microsurgery laser while the cells closest to the target remain intact. Because the targeted cell is completely embedded in collagen, which restrains the motion of cells in 3D, these experiments show that the immediate loss of fluorescence upon irradiation is due to ablation at the cell and not displacing the cell out of the FOV.

3. Discussion

The single-pulse cellular ablation demonstrated with the TPM/FLMS probe in Fig. 3 compares well to cellular ablation studies conducted using high-NA table-top systems [1, 4, 33]. To compare between these studies, we can estimate peak intensities based on the focused spot size and the reported pulse duration. The spot size at the focal plane of our probe is ~3.8 μm, as calculated by multiplying the $1/e^2$ width of the measured PSF by $\sqrt{2}$, because the PSF represents the intensity-squared distribution. Thus, the 280 nJ pulse energy used for ablation corresponds to a peak laser intensity of 14 TW/cm^2 when accounting for the spot size of ~3.8 μm and the pulse duration of ~178 fs. This intensity is comparable to the 9.6 TW/cm^2 single-pulse ablation threshold that we have found for nanosurgery in *C. Elegans* using a 1.4-NA objective lens [33].

#95706 - $15.00 USD Received 2 May 2008; revised 8 Jun 2008; accepted 10 Jun 2008; published 20 Jun 2008

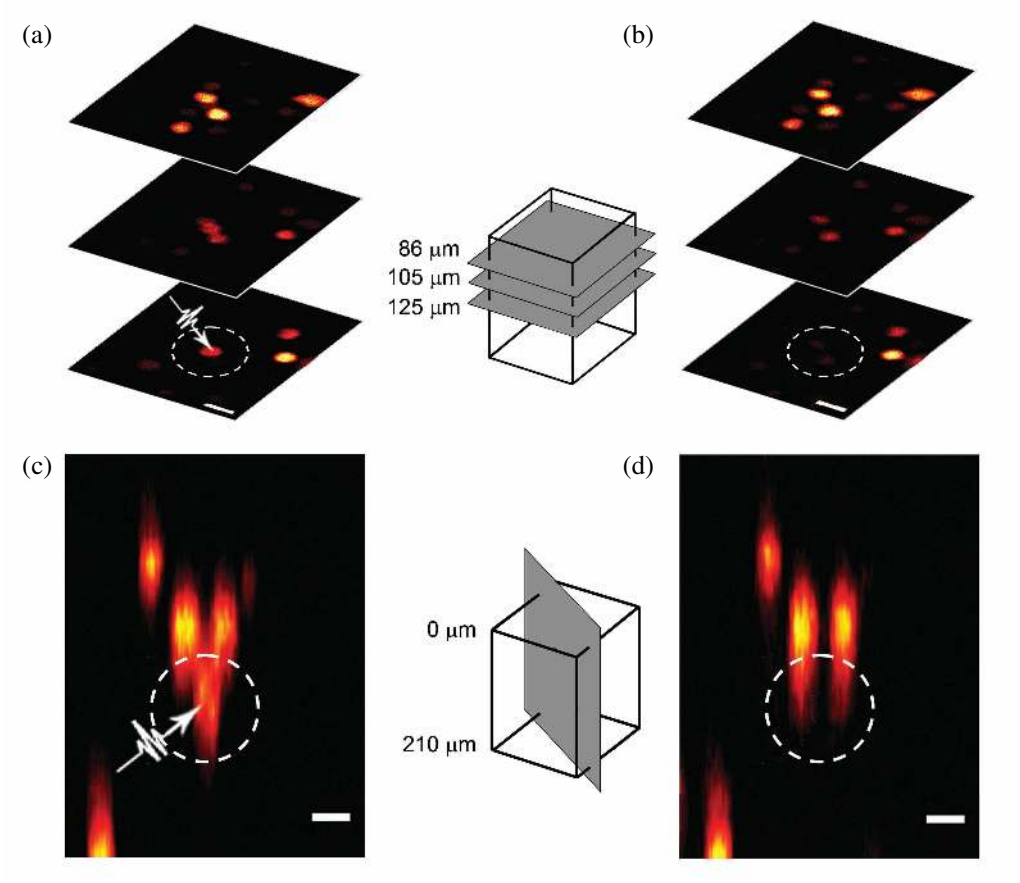

Figure 4. Combined two-photon microscopy and femtosecond laser microsurgery of breast carcinoma cells in a collagen tissue phantom. (a) Lateral slices with FOV of 116 × 160 µm^2 depicting a cell targeted for ablation as well as cells above it. The distance between the center of the targeted cell and those of the two cells above it is ~35 µm. (b) The same cells shown in (a) after irradiation of the targeted cell with 5000 pulses at 213 nJ pulse energy. (c, d) Vertical slice reconstruction through the same targeted cell and the cells above it before and after laser irradiation, respectively. Total imaging depth was 210 µm and the axial spacing between lateral slices was 6.6 µm. Scale bars are 20 µm.

Also, it is well known that the threshold for femtosecond laser ablation decreases as larger numbers of pulses are used as a result of an incubation effect. For example, when the number of pulses was increased to 1,000 in our *C. Elegans* nanoaxotomy study, we observed a decrease in threshold from 9.6 TW/cm^2 to 1.8 TW/cm^2 [33]. When comparing to the multiple-pulse cellular ablation studies, Shen *et al*. [4] achieved ablation of individual mitochondria within cells with 1,000 pulses at 9.1 TW/cm^2, as estimated based on the reported NA of 1.4 using $d = 0.925\lambda/NA$ [34]. Additionally, Tirlapur and König succeeded in optoporating cells using over one million pulses at 2.4 TW/cm^2 at an 80 MHz pulse repetition rate and NA of 1.3 [1]. For comparison, during ablation within the collagen tissue phantom, the 5000 pulses at 213 nJ correspond to ~11 TW/cm^2 per pulse. Given the scattering that occurs within the turbid tissue-like media of the phantom, the intensity used in this experiment compares well to the intensities used in other multiple-pulse experiments. In light of these results for both single- and multiple-pulse experiments, the observed cellular ablation threshold using the TPM/FLMS probe suggests that we were able to achieve femtosecond laser microsurgery with efficiency comparable to high-NA table-top systems.

#95706 - $15.00 USD Received 2 May 2008; revised 8 Jun 2008; accepted 10 Jun 2008; published 20 Jun 2008

Furthermore, the laser dosages used here for two-photon imaging are estimated to be at a safe level for cell vitality, which is crucial for sensitive clinical applications (see Table 1). Cell viability will depend on both the incident peak laser intensity and the number of pulses at this intensity that the cell receives. Thus for comparison, the number of overlapping consecutive pulses was estimated as well as the peak intensity. The number of overlapping pulses is defined here as the laser repetition rate divided by the product of the spot size and the scanning speed. For the probe, the slow axis MEMS scanning frequency and the ~116 μm FOV of this experiment were used to arrive at a conservative estimate of scanning speed. Looking at peak intensity, the maximum average power used during cell imaging (17 mW used for imaging in the tissue phantom) corresponds to a peak intensity at the sample of ~13 GW/cm^2, which is below the maximum peak intensities found to be safe for long term two-photon imaging in recent studies [35-38]. In addition, the fast scanning speed used in the probe results in far fewer consecutive pulses delivered per spot at this intensity, which further reduces the overall laser dosage to the sample when imaging with the probe. The favorable comparison shown in Table 1 indicates that the collection efficiency of the probe is sufficiently high to enable safe cellular two-photon imaging using conventional fluorophores.

Table 1. Comparison of imaging conditions proven not to affect cell viability to imaging conditions used in this study.

	Other studies presenting threshold imaging conditions that do not impair normal cell function				
	König *et al.* [35], 1997	König *et al.* [36], 1999	Koester *et al.* [37], 1999	Hopt and Neher [38], 2001	This study
Peak Intensity [GW/cm^2]	34	61	78	27	13
Number of overlapping pulses while scanning	53,000	8,500	15,000	2,800	850

4. Conclusion

In conclusion, we have developed a miniaturized TPM/FLMS probe that can perform microsurgery through precise femtosecond laser ablation and provide visualization of the operation region through two-photon imaging. This miniaturized probe measures only 10 × 15 × 40 mm^3 and serves as a flexible test bench towards development of a clinical TPM/FLMS endoscope. Imaging is accomplished by Lissajous scanning a two-axis gimbal MEMS mirror while microsurgery is accomplished using prechirped femtosecond laser pulses with energies up to 280 nJ through an air-core PCF.

Future design improvements such as a metallic-coated high reflectivity MEMS mirror and a high-NA miniature objective lens, which will provide increased power delivery and improved collection efficiency, respectively, can enable imaging of cellular autofluorescence with the probe. An increase in numerical aperture will also be beneficial for precise FLMS inside bulk tissue, where tighter focusing can help to reduce the pulse energy and avoid collateral damage arising from nonlinear affects [3]. Meanwhile, novel two-photon contrast agents, such as bright luminescent gold nanorods, can be used to reduce the required excitation power by a couple of orders of magnitude in addition to providing molecularly specific imaging [39, 40]. Improvements in axial resolution would also improve optical sectioning, and could allow for 3D imaging of tissue if paired with a mechanism for axial scanning. Several such systems have been devised, including translating individual components or the system by a micromotor, piezoelectric actuator, or MEMS device for fully automated three-dimensional imaging [20, 41]. These improvements, combined with further

#95706 - $15.00 USD Received 2 May 2008; revised 8 Jun 2008; accepted 10 Jun 2008; published 20 Jun 2008

miniaturization through the use of smaller-diameter relay optics and optimized packaging, can lead to a powerful clinical TPM/FLMS device.

Fiber-coupled systems with near-video rate imaging and high precision surgery capabilities such as the one presented here can be used for live animal studies for developing clinical techniques. The optical design approach presented in this paper shows great promise and could find applications in such disparate fields as oncology, dermatology, and neurosurgery.

Acknowledgments

The authors would like to acknowledge Daniel Eversole and Dr. Frederic Bourgeois for assistance with cell culturing and Sam Guo and Rick Harrison for assistance with SEM imaging. The authors would also like to thank Prof. Ofer Levi for valuable discussions. N. D. is partially supported by a National Science Foundation IGERT Fellowship. This work was funded by National Science Foundation grants BES-0548673 and BES-0508266 and National Institute of Health grant R03-CA125774.

#95706 - $15.00 USD Received 2 May 2008; revised 8 Jun 2008; accepted 10 Jun 2008; published 20 Jun 2008